Journal of Thermal Biology 86 (2019) 102433

Contents lists available at ScienceDirect

Journal of Thermal Biology

journal homepage: http://www.elsevier.com/locate/jtherbio

The effect of small-scale morphology on thermal dynamics in coral microenvironments

Robert H. Ong [a], Andrew J.C. King [b,c], Benjamin J. Mullins [b,d,*], M. Julian Caley [e,f]

[a] Centre for Wind, Waves and Water, School of Civil Engineering, The University of Sydney, Darlington, NSW, Australia
[b] Fluid Dynamics Research Group, Curtin Institute for Computation, Department of Mechanical Engineering, Curtin University, Perth, Australia
[c] School of Civil and Mechanical Engineering, Curtin University, Bentley, WA, Australia
[d] Occupation and Environment, School of Public Health, Curtin University, Bentley, WA, Australia
[e] School of Mathematical Sciences, Queensland University of Technology, QLD, Australia
[f] Australian Research Council Centre of Excellence for Mathematical and Statistical Frontiers, VIC, Australia

ARTICLE INFO

Keywords:
Micro-scale morphology
Polyp thermal dynamics
CFD
Coral microenvironments

ABSTRACT

The thermal microenvironments of corals is a topic of current interest given their relationship to coral bleaching. We present computational fluid dynamics (CFD) model of corals with both smooth and rugged polyp surface topographies for two species of massive corals (*Leptastrea purpurea* and *Platygyra sinensis*) in order to predict their microscale surface warming. This study explores whether variation in polyp depth (*PD*) may directly effect a coral overall surface area-to-volume (A/V) ratio and consequently its surface warming. Validation of our models was made against detailed laboratory measurements of coral surface warming and thermal boundary layer thickness. Our results suggested that while differences in surface warming exist between smooth surfaces and surfaces covered in micro-polyps (5 mm depth), the variation in terms of surface warming is small (~0.18–0.19°C) and it can be largely attributed to increasing A/V ratios. Our results demonstrated good agreement with measurements of surface temperatures on living corals and that ignoring the presence of polyps by modelling heat transfer associated with a smooth surface makes no material difference to the values obtained or the interpretation of the processes leading to surface warming.

1. Introduction

Coral reefs provide extensive ecosystem goods and services to tropical and subtropical nations (Moberg and Folke, 1999). However, major coral bleaching events have caused widespread coral mortality over the past few decades (Glynn, 1990, 1996; Hoegh-Guldberg, 1999), and thereby, threaten the ongoing supply of these goods and services. Spatial and temporal variability in the bleaching dynamics varies as a consequence of local sea surface temperature (SST) variation (Teneva et al., 2012), levels of irradiance experienced by corals (Mumby et al., 2001; Dunne and Brown, 2001), water flow around coral colonies (Nakamura et al., 2003, 2005; Fabricius, 2006; Jimenez et al., 2008), and the morphology of coral colonies (Loya et al., 2001; Marshall and Baird, 2000; van Woesik et al., 2012). Coral morphology, a colony's size, shape, and composition with respect to tissue thickness and permeability of coral colonies, best explains observed variations in bleaching susceptibility (Shenkar et al., 2005; Brandt, 2009; Guest et al., 2012; Jimenez et al., 2011). Variation in coral morphology, however, is confounded by coral systematic as morphology is strongly conserved among large groups of coral species and ranges from highly complex branching structures to simple hemispherical and encrusting forms (Veron, 1995, 2000).

Despite the potential importance of coral thermal microenvironments to the thermal energy budgets of corals and other physiological processes, only a few studies have considered the actual temperature of corals and the heat fluxes at their surfaces. Fabricius (2006) measured the surface temperature of a number of shallow-water corals and showed that more densely pigmented corals heated more than less densely pigmented ones, an effect that was enhanced under low water flow conditions. Jimenez et al. (2008) also detailed the heat budget of a coral exposed to solar radiation and water flow under controlled experimental conditions and on a reef flat under naturally fluctuating conditions of

* Corresponding author. Fluid Dynamics Research Group, Curtin Institute for Computation, Department of Mechanical Engineering, Curtin University, Perth, Australia.
E-mail address: b.mullins@curtin.edu.au (B.J. Mullins).

https://doi.org/10.1016/j.jtherbio.2019.102433
Received 25 May 2019; Received in revised form 10 August 2019; Accepted 6 October 2019
Available online 11 October 2019

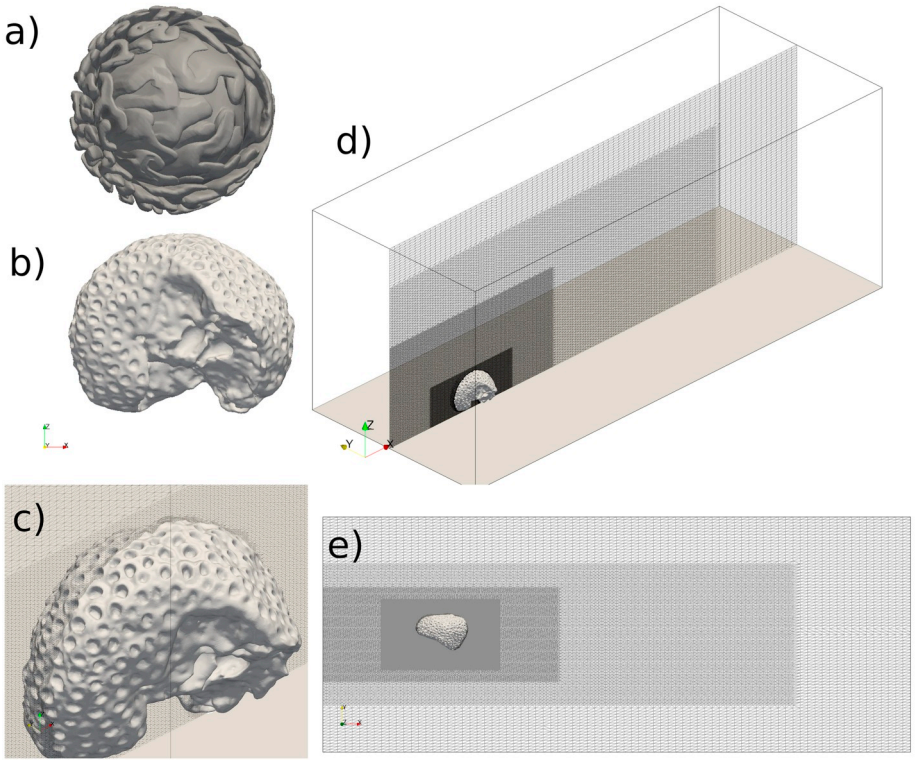

Fig. 1. Conceptual representations of geometrical characteristics for both model species used in Jimenez et al. (2011). **(a)***P. sinensis* and **(b)** *L. purpurea*, **(c–e)** the adopted mesh refinement of the computational domain showing the cell size compared to the boundary layer thickness of the coral.

Table 1
Initial and boundary conditions used to model conditions of the apparatus used by Jimenez et al. (2011), where S: slip, ZG: zero gradient, ZNG: zero normal gradient, FV: fixed value.

Parameter (units)	Initial value	Surrounds	Floor	Inlet	Outlet
reference pressure	atmospheric	S	ZG	ZG	FV
velocity (u)	0.01 m s^{-1}	S	ZG	FV	ZNG
temperature (T)	25 °C	S	FV	FV	ZG

Table 2
Comparison of the actual and estimated surface area and volume.

Shape	Size (m)	Actual		Model		RMSE	
		A (m^2)	V (m^3)	A (m^2)	V (m^3)	A (m^2)	V (m^3)
Hemisphere	0.5	0.39	0.033	0.41	0.033	0.020	4×10^{-4}
Cylinder	0.3	0.283	0.011	0.262	0.012	0.021	0.002

flow and irradiance. These experimental studies provided the first evidence that the thermal microenvironment can play an important role in the microscale processes involved in coral bleaching. In order to better understand such relationships between water temperature and coral morphology, we previously developed and validated a heat transfer model that was coupled with fluid dynamics to study coral thermal microenvironments under controlled laboratory conditions (Ong et al., 2012). Our approach using computational fluid dynamics (CFD) models allowed us to study different coral species, morphologies and pigmentations and model the thermal microenvironments of the corals under various water-flow velocity and irradiance level.

Corals are modular organisms in which each coral colony consists of numerous, interconnected, genetically identical modules, the polyps. Given the intricacy of modelling this micro-polyp scale architecture, achieving realistic levels of texture detail is currently beyond the capabilities of available medical scanners and computer-aided-design (CAD) software. As is generally the rule for biophysical models, our previous mechanistic approach was a simplified representation of a biological system. In particular, polyp architecture was not considered and only the key controlling processes were modelled. The biophysical model we used in our previous study imposed a simplistic coral structure with smooth surface topographies, and a uniform tissue layer covering the skeleton. By adopting such an approach, we viewed these colonial organisms as integrated wholes rather than structured collections of small polyp (Ong et al., 2012, 2017). Here we extend the work of Ong et al. (2012) by analysing the effects of coral surface topography and outlining the potential contributions of surface area-to-volume (A/V) ratios at different polyp depths (PD) to micro-polyp scale processes in influencing the thermal dynamics of coral microenvironments. The A/V ratio is an essential parameter in determining the thermal and mechanical properties of differently shaped and sized morphologies and has many other important implications in biology (e.g. thermal regulation and metabolic scaling with body shape and size). A previously published study that explored the effects of convection and boundary layer thickness on colony morphology (i.e. Jimenez et al. (2011)) was used for validation purpose here.

1.1. Hydro and thermal physics in coral microenvironments

Typically, ambient water temperature, represented by the SST, is assumed to be the temperature experienced by corals and the best indicator of the thermal stress they experience. However, it is the temperature of the colony surface and the boundary layer directly surrounding it that determines the state and dynamics of their physiological processes (Fabricius, 2006; Jimenez et al., 2008, 2011) and this temperature may differ substantially from the temperature of the

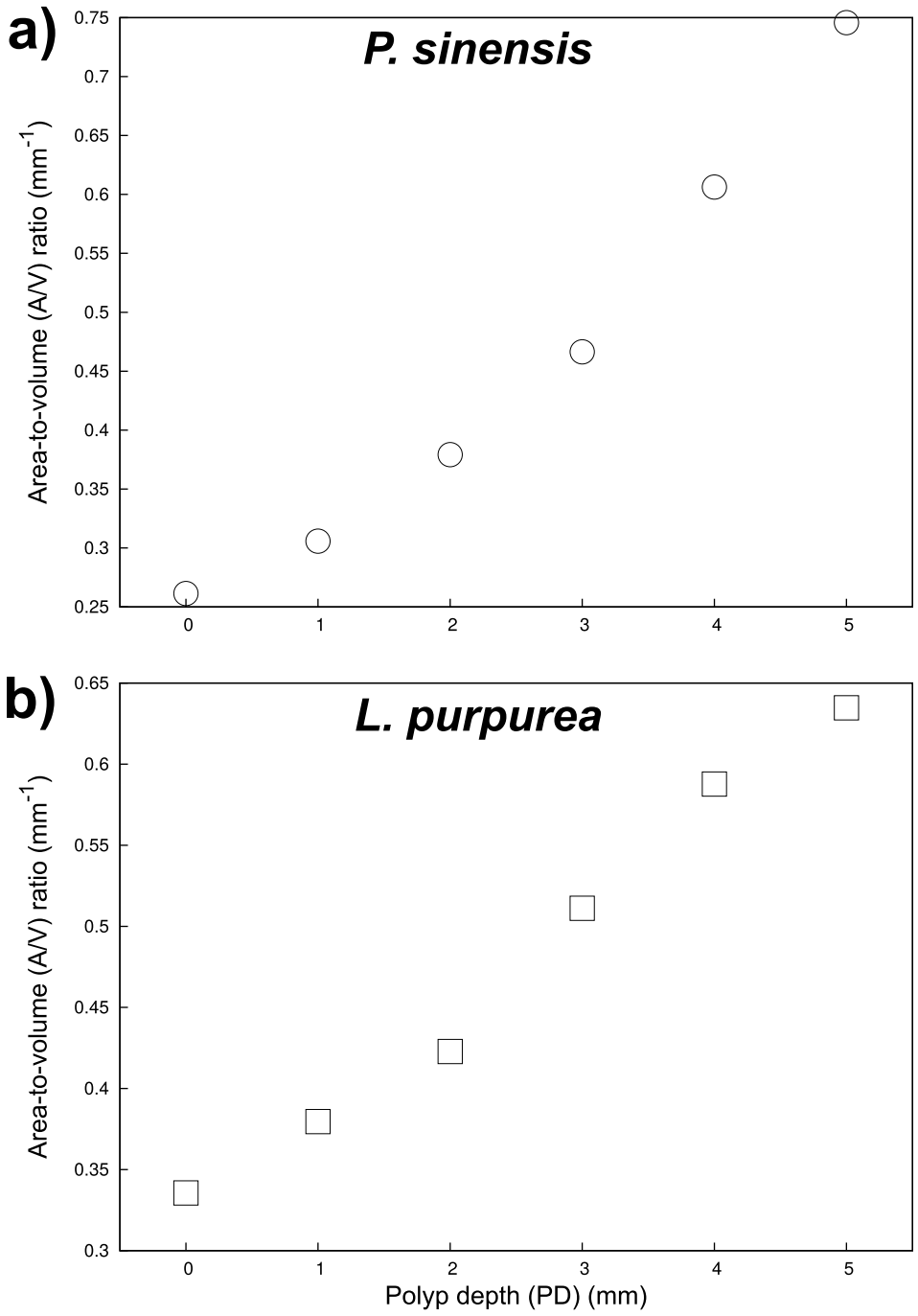

Fig. 2. The surface area to volume (A/V) ratio against polyp depth (PD) of: **(a)** *P. sinensis* and **(b)** *L. purpurea*. These points are most closely described by exponential curves.

surrounding seawater. This boundary layer and coral colony surface is collectively referred to here as the coral thermal microenvironment. This temperature difference between the surrounding seawater and a coral thermal microenvironment is a function of several factors, though it is predominantly due to radiative heat flux and water flow across the coral surface. It these factors that determine the heat balance between losses from convection into the surrounding water which is dependent on water flow and other surface characteristics involved in the boundary layer formation, heat conduction into deeper layers of the coral, and short and long-wave radiation incident on the coral surface (Fabricius, 2006; Jimenez et al., 2008, 2011; Ong et al., 2012).

Therefore, any flow of water through the coral tissue that envelops a coral colony could significantly influence its thermal microenvironment. The model we present here, however, assumes that there is unlikely to be any significant permeability through intact living tissue. The exception to this would be where the activity of borers and coral grazers result in openings that allow water percolation into and through the porous coral skeleton. Our validation case study (i.e. Jimenez et al. (2011)) used cut pieces of coral, which would have had significant permeability on their cut faces. Thus, in order to validate our modelling results against their experimental results, we have assumed 5–10% porosity (φ) in coral tissues which approximates the percentage of cut surface areas of the coral pieces in the colonies they tested.

In these porous zone models, the corals were also treated as being isotropic with uniform porosity and permeability. To describe the temperature distribution in the porous coral tissue and skeleton, we

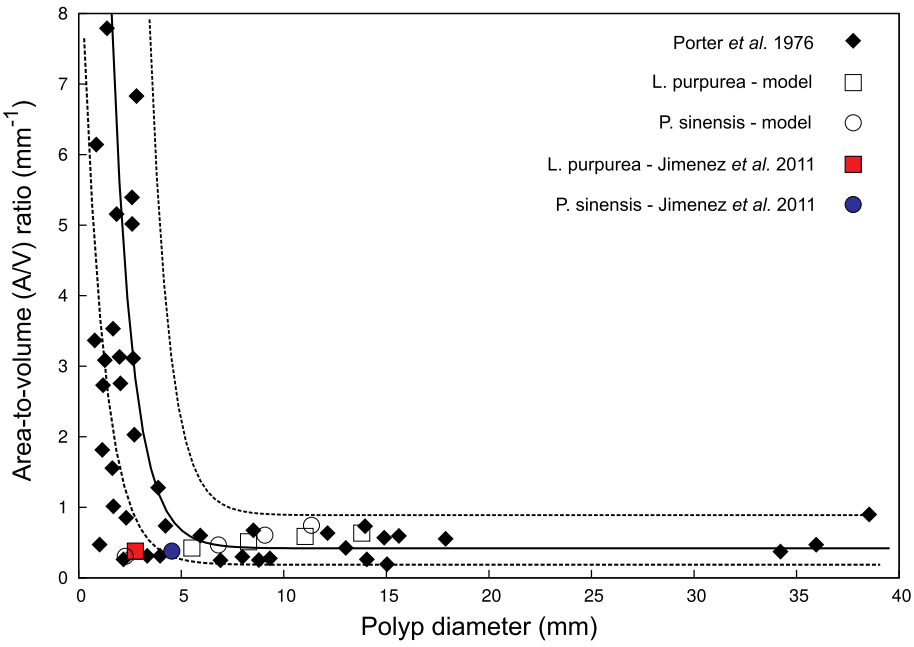

Fig. 3. The surface area to volume (A/V) ratio (mm^{-1}) against polyp diameter (mm) of *P. sinensis* and *L. purpurea* compared with Porter (1976) data for 43 species of Caribbean coral and can be described by the exponential curve $A/V = 1.9\ D^{-0.8}$ drawn as a solid line with upper and lower 95% confidence limits as dashed lines. The colored points represent the corals used by Jimenez et al. (2011), while the open squares and circles are our simulated A/V ratios for a range of polyp diameters.

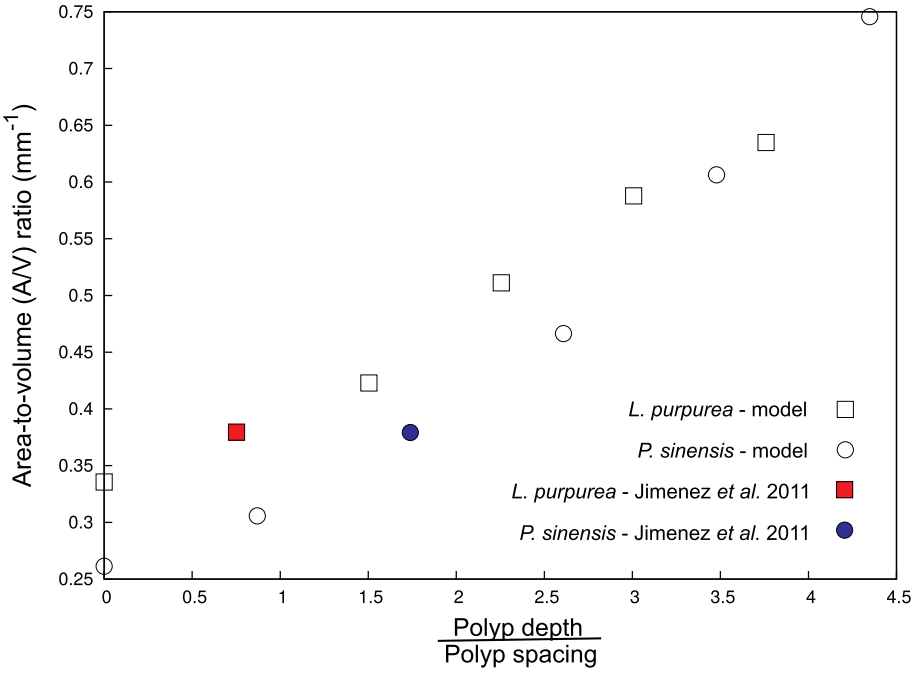

Fig. 4. The surface area to volume (A/V) ratio (mm^{-1}) against the ratio of polyp depth to polyp spacing of *P. sinensis* and *L. purpurea*.

assumed an instantaneous local thermal equilibrium: $T_c = T_f = T$, where the subscripts c and f refer to the coral and fluid phases, respectively. An overall heat balance between heating and cooling in a coral can thus be written as:

$$Q_{\text{eff. heating}} = Q_{\text{absorb}} - Q_{\text{cool}} \quad (1)$$

where Q_{absorb} is the heat absorbed by a coral due to solar irradiance and Q_{cool} is the energy that is transferred from the coral surface to the surrounding environment. Applying Newton's law of cooling and rearranging the above equation, Q_{cool} and Q_{absorb} can be expressed as:

$$Q_{\text{cool}} = hA(T_{\text{tissue}} - T_{\text{water}}) \quad (2)$$

$$Q_{\text{absorb}} = \alpha IA \quad (3)$$

where h is the heat transfer coefficient between the coral surface and the surrounding environment, I is the total irradiation, α is the tissue absorptivity, and A is the surface area of the coral. Heat transfer is directly proportional to surface area, whereas heat capacity is proportional to

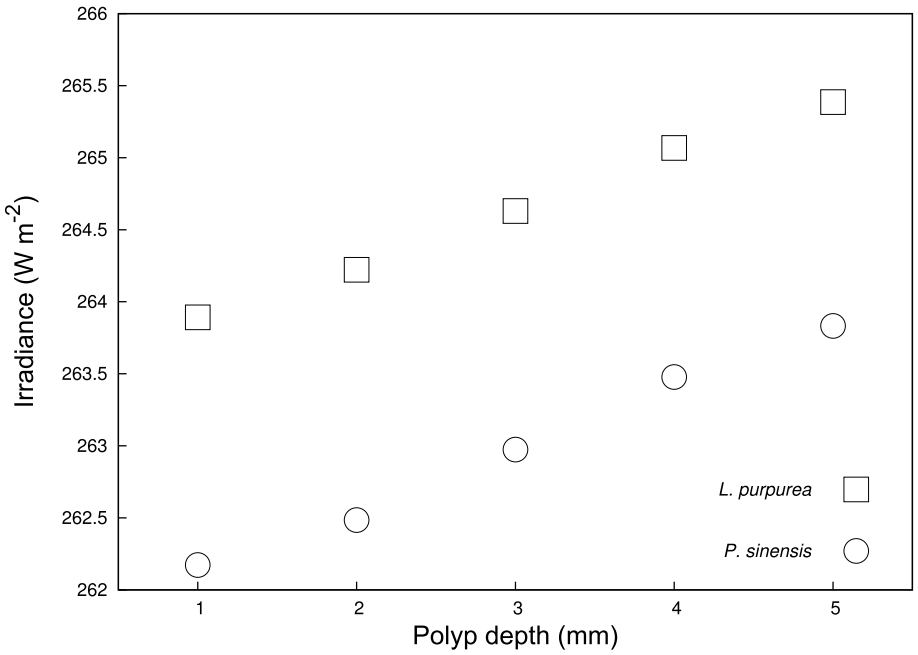

Fig. 5. Irradiance levels at the microscale of polyps as a function of polyp depth (PD) of *P. sinensis* and *L. purpurea*.

volume. Hence, the A/V ratio would be expected to influence heat accumulation and dissipation. Consequently, A/V ratios and their relationship to coral thermal microenvironments are also considered here.

2. Methods

2.1. Numerical model

This study was conducted using OpenFOAM (Computational Fluid Dynamics Software) (OpenCFD Ltd., 2010). The governing equations of fluid flow and heat transfer processes presented in this paper are expressed in differential equations written in Cartesian coordinates. The mass, momentum, and energy conservation equations are solved over all the fluid control volumes (termed as computational cell) in a computational domain using the Finite Volume Method (FVM). This solution provides results at each finite volume in the model, at discrete time intervals (for further readings on FVM, the reader is referred to (Ferziger and Perić, 1999; Versteeg and Malalasekera, 1995)).

The physical laws governing porous media, fluid flow, and heat transfer processes must firstly be defined as differential equations. The mass continuity governing equation was developed from the mass balance over a control volume (cell), fixed in space, through which the fluid flows is given by:

$$\frac{\partial \rho}{\partial t} + \nabla \cdot (\rho \mathbf{U}) = 0 \tag{4}$$

where **U** is the superficial velocity vector. Because the present model is at the laboratory scale, any differences in seawater density will be very small, and are therefore ignored, and fluid flow is treated as being incompressible. However, the application of this modelling framework at larger scales, will require these assumptions to be re-visited because changes in density are likely with changes in salinity and temperature.

The momentum governing equation for laminar, viscous, incompressible, single-phase water flow through a porous medium is given by:

$$\frac{\partial}{\partial t}(\phi \mathbf{U}) + \nabla \cdot (\mathbf{U} \cdot \mathbf{U}) = \nu \nabla^2 \mathbf{U} - \frac{\nabla p}{\rho} + S_i \tag{5}$$

where ϕ is porosity, ν is kinematic viscosity, p is pressure, and k is thermal conductivity. The flow sink term, S_i is composed of two parts, a viscous loss term and inertial loss term, creating a pressure drop that is proportional to the velocity and square of the velocity, respectively.

$$S_i = -\left(\nu D_{ij} + \frac{1}{2}|\mathbf{U}|F_{ij}\right)\mathbf{U} \tag{6}$$

where D_{ij} and F_{ij} are represented as the scalars D and F. This is the classical Darcy-Forchheimer equation. In this study, corals were assumed to possess homogeneous permeability and were treated as having isotropic permeability. The Blake-Kozeny equation specifies viscous energy loss primarily in laminar flow as:

$$D = \frac{150(1-\phi)^2}{d^2\phi^3} \tag{7}$$

where, d is the diameter of the coral sample under investigation. The Burke-Plummer equation denotes the kinetic energy loss primarily in turbulent flow as:

$$F = \frac{1.75(1-\phi)}{d\phi^3} \tag{8}$$

The averaged momentum equation for steady, turbulent incompressible flow can be written as:

$$\frac{\partial}{\partial x_j}\left(\overline{u_j u_i}\right) = -\frac{\partial}{\partial x_i}\left(\frac{\overline{p}}{\rho}\right) + \frac{1}{\rho}\frac{\partial}{\partial x_j}\left(\tau_{ij} + \tau_{t_{ij}}\right) - \overline{S_i} \tag{9}$$

The final transport equation is the energy governing equation, which accounts for heat flow within the models, including the effects of incident solar radiation. In the porous zone models, we treated all the corals as isotropic media with uniform porosity and permeability. Although this may not be realistic in some cases, we consider this to be a reasonable starting approximation. To describe the temperature distribution in the porous coral tissue and skeleton, we assumed an instantaneous local thermal equilibrium whereby $T_c = T_f = T$ (where T_c and T_f are the temperatures of the coral and the fluid, respectively). It can be expressed as:

$$\left(\rho C_p\right)_m \frac{\partial}{\partial t} T + \left(\rho C_p\right)_m \nabla \cdot \mathbf{U} T = \nabla \cdot (k_m \nabla T) + S_h \tag{10}$$

where S_h accounts for heat source (such as the incident radiation on the

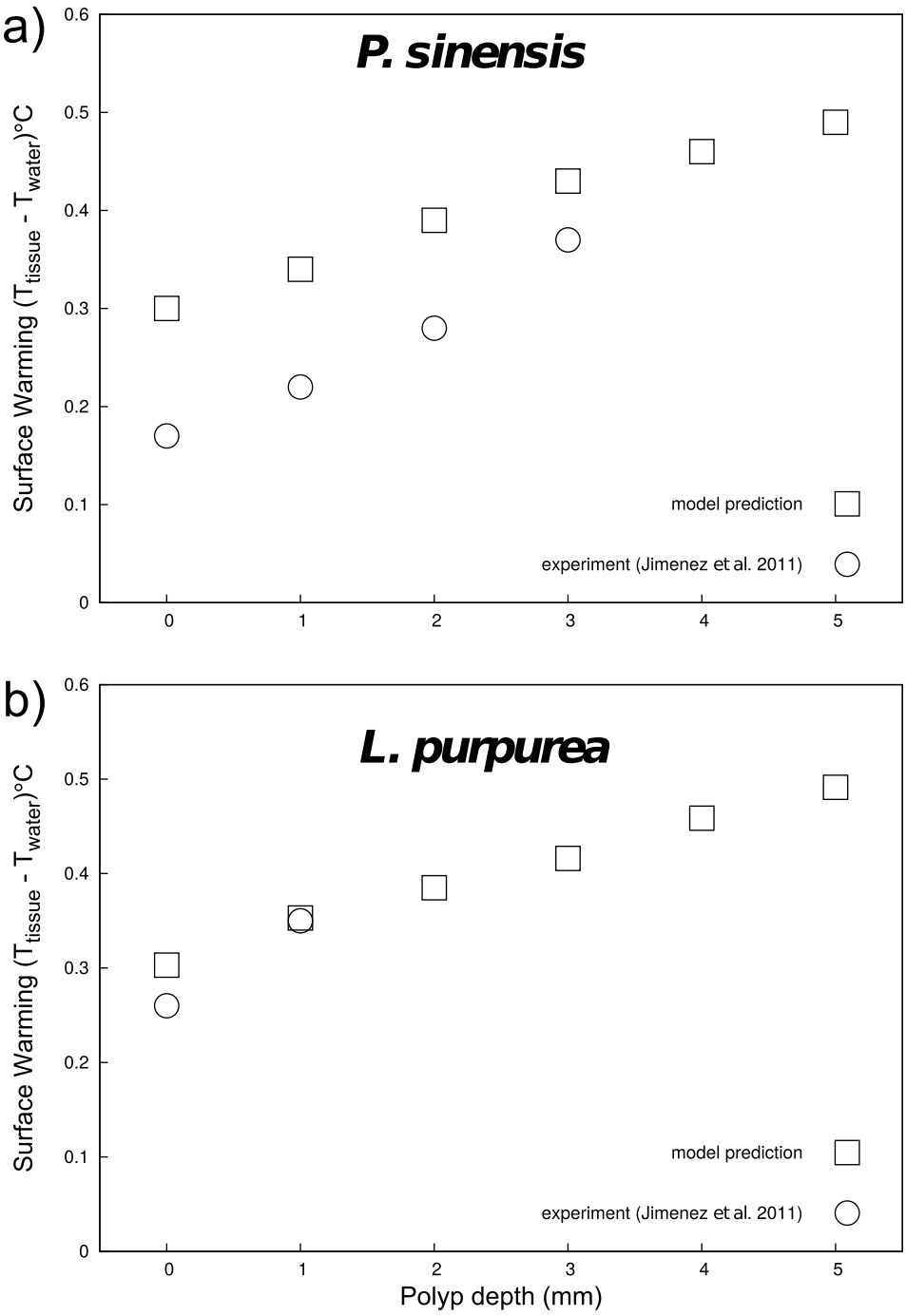

Fig. 6. Comparisons of observed and modelled warming of polyp surfaces over: **(a)** *P. sinensis* and **(b)** *L. purpurea* under a fixed inlet flow of 0.01 m s^{-1} heated to 430 W m^{-2}.

tissue, Q_{rad}). Averaged material properties for the porous media were calculated using:

$$\rho_{eff} = (1-\phi)\rho_c + \phi\rho_f \tag{11}$$

$$C_{p_{eff}} = (1-\phi)C_{p_c} + \phi C_{p_f} \tag{12}$$

$$k_{eff} = (1-\phi)k_c + \phi k_f \tag{13}$$

where Equations (11)–(13) represent effective density, effective heat capacity, and effective thermal conductivity of the medium, respectively. These values were then used to calculate the thermal diffusivity of the medium, Γ_{T_m}, which is given by:

$$\Gamma_{T_m} = \frac{k_m}{(\rho C_p)_m} \tag{14}$$

The source term added to the energy equation needs to be modified to have the same dimensions as the other terms. The absorbed heat irradiance to each cell in coral tissue in contact is $\dot{q}\cdot A$ [J s^{-1}]. The other terms in the energy equation has the dimensions of [J s^{-1} m^{-3}] before dividing by $(C_p\cdot\rho)$. Therefore the source term needs to be divided with the cell volume of the corresponding cell in order to obtain the correct dimension.

The overall heat transfer parameters are highly dependent on the geometry and density of the corals. Dividing equation (10) by the $(\rho C_p)_m$

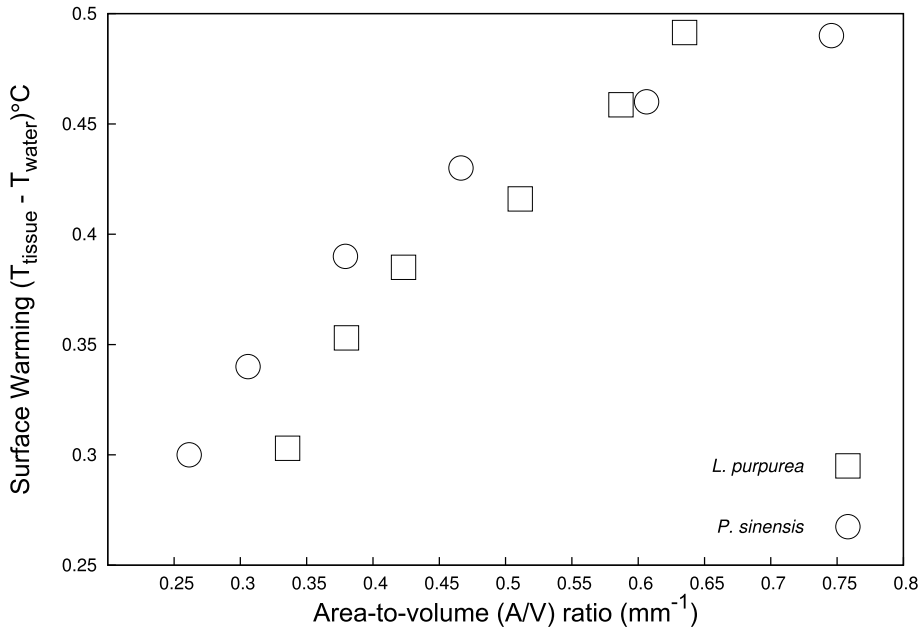

Fig. 7. Plot of the A/V ratios against coral surface warming under a fixed inlet flow of 0.01 m s^{-1} heated to 430 W m^{-2}.

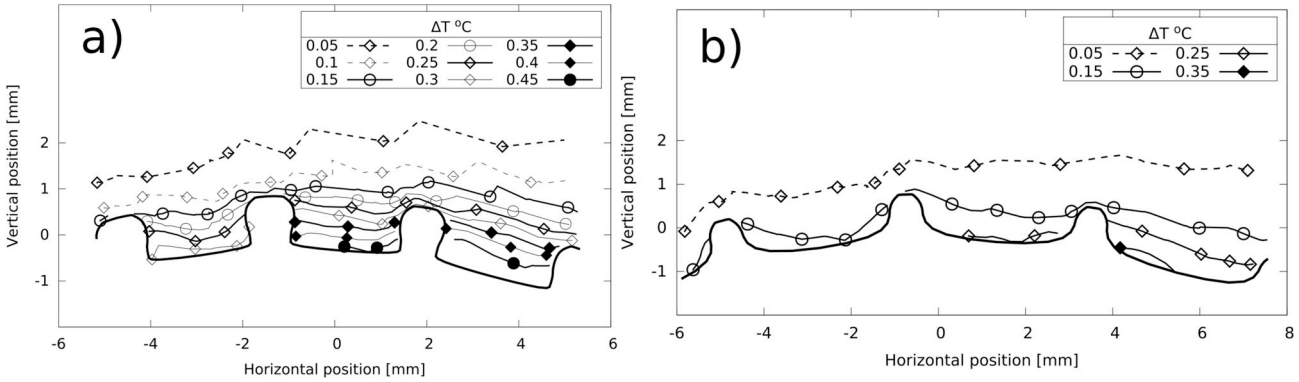

Fig. 8. Modelled contour of surface warming over two neighbouring polyps for **(a)** *P. sinensis* and **(b)** *L. purpurea*, under flow of 0.01 m s^{-1} heated to 430 W m^{-2}.

term yields a more standardised transport energy equation for porous media given as

$$\frac{\partial}{\partial t}T + \nabla\cdot\mathbf{U}T = \Gamma_T\nabla^2 T + \frac{\Gamma_T}{k}S_h \tag{15}$$

The angle of incidence (θ) and intensity (Q_{rad}) of solar radiation that strikes the coral's surface (tissue) is also accounted for in the model. However, for the purpose of validating the models against experimental measurements, the Q_{rad} term was calculated using an overhead (90°) incident angle for solar radiation delivered to the tissue surface. Hence, Equation (15) can be written as:

$$\frac{\partial}{\partial t}T + \nabla\cdot\mathbf{U}T = \Gamma_T\nabla^2 T + \frac{\alpha Q_{rad}}{\rho C_p} \tag{16}$$

The heat transfer energy equation in the incompressible turbulent flow remains unchanged as the above with the additional viscous dissipation term added on the right hand side of the equation. This term is important only in flows with big velocity gradients, which is not the case here and thus, it is expected to be negligible when determining the temperature. The turbulent heat dissipation can be written as:

$$(\overline{\mathbf{U}}\cdot\nabla T) = \frac{k\nabla^2 T}{\rho C_p} + (\tau : \nabla\overline{\mathbf{U}}) \tag{17}$$

When a fluid flows over a surface, its first layer normally sticks to the boundary (no slip boundary condition). This phenomenon causes the flow to decrease, in this case, in the vicinity of the bounding coral surface, creating the hydrodynamic boundary layer. A similar principle applies when the temperature between the fluid and surface differ. The first layer of the fluid obtains its heat from the coral surface through pure conduction. It then gives its newly acquired energy to all of the other fluid molecules through convection with which it comes in contact. This layer between the fluid and the bounding coral surface is called the thermal boundary layer. In this work, Equations (5) and (16) directly account for these boundary layers based on the ascribed boundary conditions. The ratio of the thermal vs hydrodynamic thicknesses is given by the Prandtl number:

$$Pr = \frac{\text{Viscous Diffusion Rate}}{\text{Thermal Diffusivity}} = \frac{\nu}{\Gamma_T} \tag{18}$$

where Γ_T is thermal diffusivity, α is coral absorptivity, ρ and C_p are the effective density and heat capacity of coral and water, and Q_{rad} accounts for heat source (the incident radiation on the tissue). Hence, a Prandtl number greater than 1 indicates that momentum diffusion is the more dominant process resulting in a slightly thinner thermal boundary layer (TBL) compared to the momentum boundary layer (MBL).

In laminar flow, the flow behaves as if it were nearly inviscid over

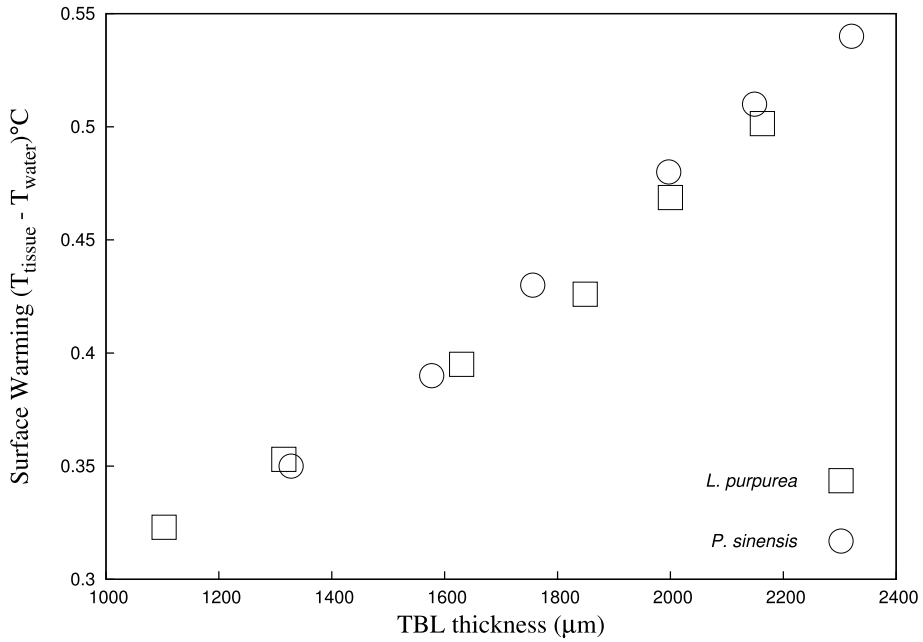

Fig. 9. Coral surface warming plotted against the thermal boundary layer thickness (μm) under a water flow of 0.01 m s^{-1} heated to 430 W m^{-2}.

most of the domain, with viscous and diffusive effects only becoming important in a thin region near the substrate due to the no-slip condition, whereby there exists MBL and TBL, respectively, with thicknesses denoted by δ and δ_T. Energy transport within the TBL occurs predominantly by conduction, convection, and heat irradiance, hence the numerical prediction of surface warming can be defined as a function of the heat irradiance (Q), the absorptivity of coral tissue (α), and the convective heat transfer coefficient (h), as described in Equations (1)–(3). Both the momentum and thermal boundary layer thicknesses are obtained by plotting the heights of points at which the velocity and temperature drops to 99% ($u/U_0 > 0.99$) of its free stream values.

2.2. Model validation

We used experimental boundary layer measurements collected in a flow chamber for coral colonies of two species by Jimenez et al. (2011) to validate our CFD models. The two coral species used in their experiment, both with massive morphologies, were *Leptastrea purpurea*, (colony dimensions: diameter ~35 mm, depth: ~1 mm, and ~1.3 mm spacing) and *Platygyra sinensis*, (colony dimensions: diameter ~45 mm, depth: ~2 mm). As discussed above, corals consist of two distinct regions: an almost impermeable layer of tissue covering the surface of the colony and a highly porous calcareous skeleton. Each of these regions possess slightly different thermal properties. Because the validation case study (i.e. Jimenez et al. (2011)) used corals that would likely have had significant permeability on their cut faces, we structured our models to account for this combination of porous and non-porous surfaces. Furthermore, our model assumed the effect of metabolic mass transfer, the heat generated due to photochemical conversions, on the overall coral surface warming to be negligible (Cooper, 2008).

Jimenez et al. (2011) used a flow chamber, 10 cm high, 5 cm wide, and 25 cm long with a sand covered floor maintained at a steady flow of 0.01 m s^{-1} and an ambient temperature of 25°C. They provided irradiance from a fixed heat source set to 1500 μmol photons m^{-2}s^{-1} (~430 W m^{-2}). They then constructed temperature contour maps using microsensors from multiple temperature micro-profiles measured along a transect across a single polyp and perpendicular to the direction of water flow (Jimenez et al., 2011). To simulate the conditions used by Jimenez et al. (2011), we constructed the three-dimensional coral geometries as closely as possible with the shapes and dimensions of the colonies they used, with the aid of computer-aided-design (CAD) software (Fig. 1). The low Reynolds numbers estimated for their experimental setup indicated laminar flow conditions (~350–450).

We configured the polyped architecture as dimples arranged in each of the streamwise and spanwise directions with dimple spacing of approximately 1.2 mm. This partitioned arrangement also included the coenosteum, the area of coral skeleton covered by the live tissue known as the coenosarc. Because we modelled dimples as protruded depressions, by changing dimple depth, spacing also changed. This feature of the model also captures well the natural variation found in nature. Deep polyps tend to have wide mouths, while shallow polyps tend to have small mouths. In this study, we maintained constant dimple depth to diameter ratios for *L. purpurea* and *P. sinensis* of approximately 0.44 and 0.27, respectively. These morphological attributes of polyps will directly impact a coral A/V ratio, which can have direct impact on the photosynthetic surface area for the smaller branching corals more than large corals and are therefore favoured in light capture.

We numerically estimated the physical traits of corals (surface area and volume) by implementing a cell looping technique that simultaneously calculates and increments cell area and volume using modelled mesh-based geometries. The root mean square error (RMSE) was used to measure the difference between values predicted by the model and the theoretical calculations.

2.3. Numerical simulations

The magnitude of net irradiance absorbed by an area of coral surface is a function of the coral spectral properties such as reflectivity and transmissivity which, in turn, is determined predominantly by its darkness and orientation to the heat source. The absorptivity values for both coral species studied here were set at 0.5 following the experimental results of Jimenez et al. (2011). A thermal conductivity of seawater of 0.62 W m^{-1} K^{-1} was used, and of tissue (mesoglea) 0.22 W m^{-1} K^{-1} (Joshi, 2013), and the skeleton (aragonite) was set to 2.1 W m^{-1} K^{-1} (Ong et al., 2012). The heat balance of the coral was then modelled as a function of the losses from convection into the surrounding water, conduction from the tissue into the coral skeleton, and the emission of heat radiation. These computed values of absorbed net irradiance were subsequently converted into volumetric heat flux values via the energy term (Equation (15)), thereby taking into account both

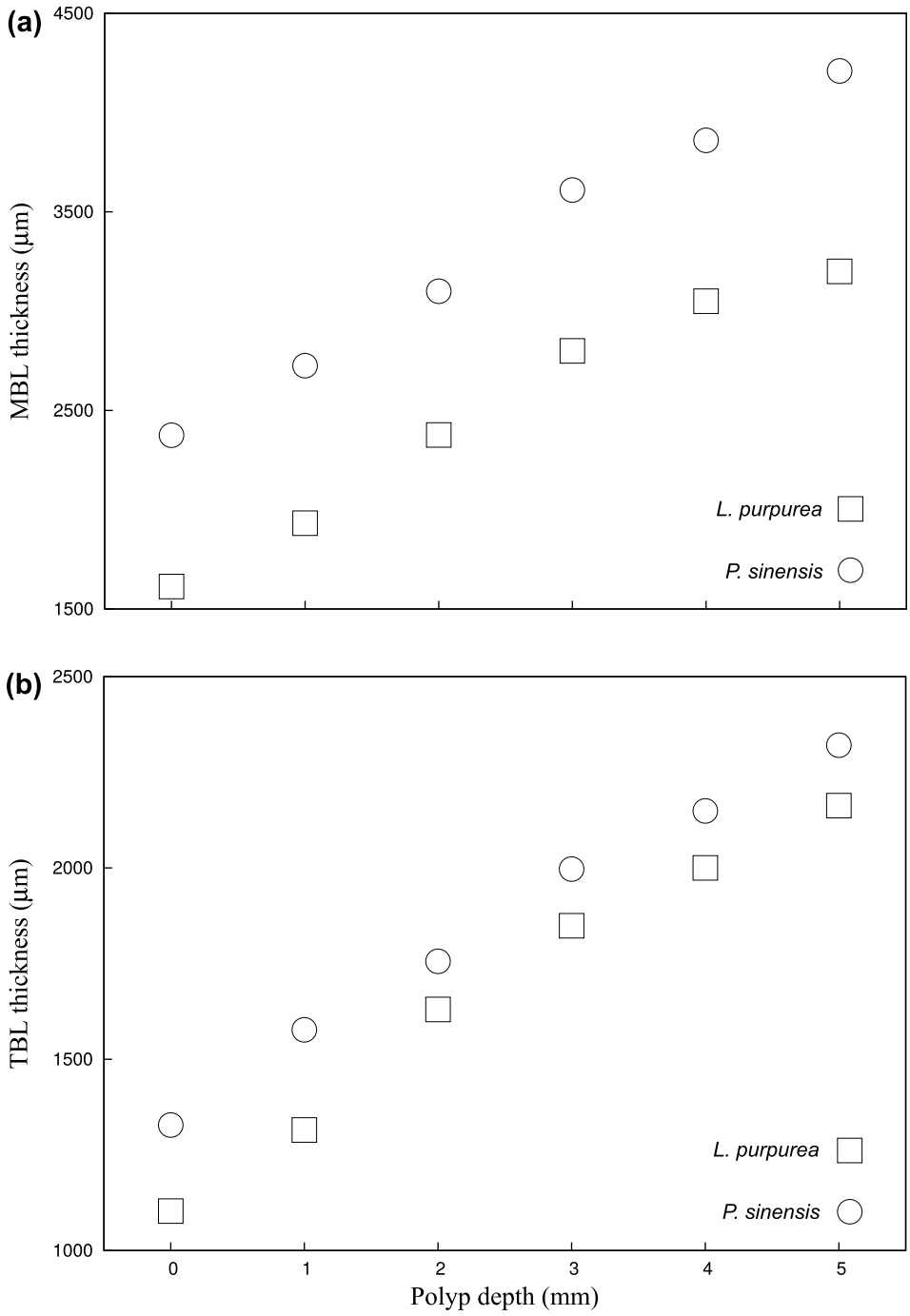

Fig. 10. The thicknesses of: (a) momentum and (b) thermal boundary layers plotted against corals (MBL and TBL, μm) over *P. sinensis* and *L. purpurea* under a fixed inlet flow of 0.01 m s^{-1} heated to 430 W m^{-2}.

the gains and losses of heat at the coral surface.

Boundary and initial conditions were also set to closely resemble the experimental conditions set by Jimenez et al. (2011). Consequently, a fixed-value boundary conditions for superficial velocity of 0.01 m s^{-1} was applied at the inlet. A zero-gradient boundary condition constrains the normal gradient of the boundary patch to zero, while the slip boundary condition sets the normal velocity component to zero. The pressure at the inlet of the apparatus was fixed at the zero gradient condition. The pressure at the outlet was fixed at the reference pressure, while the outlet velocity was fixed at the zero gradient. The velocity and pressure at the domain sides was fixed at the slip boundary condition. The initial and boundary conditions for velocity, pressure, and temperature are shown in Table 1.

The governing equations of fluid flow and heat transfer along with the aforementioned boundary conditions were solved numerically using the SIMPLE algorithm which solves for the pressure-velocity coupling (Patankar, 1980; Ferziger and Perić, 1999). The resulting system of algebraic equations is solved using the Gauss-Seidel iterative technique. A grid sensitivity analysis based on Richardson Extrapolation which aims to reduce truncation error and determine grid independent solutions were performed previously (Ong et al., 2012). The mesh near the coral was finer than anywhere else in the domain in order to adequately capture the momentum and thermal boundary layers. We used two types of grids, predefined block structured hexahedral and polyhedral, to

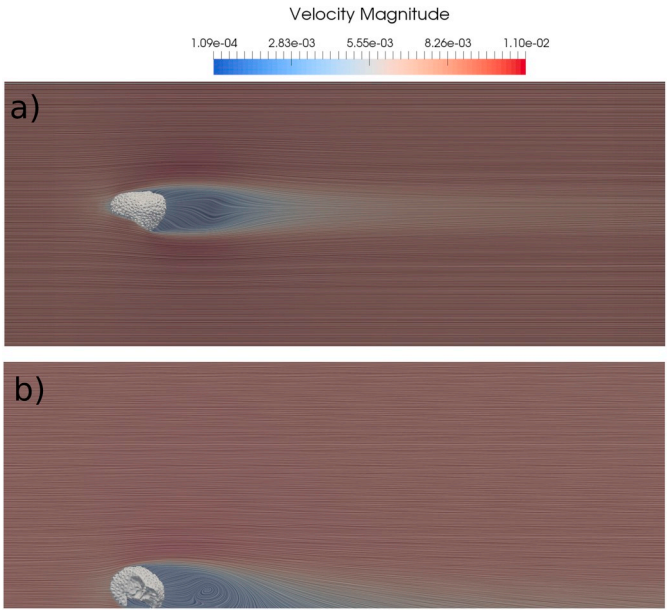

Fig. 11. Slices of streamwise flow for 5 mm dimple cross sectional planes. The inlet boundary condition is a constant velocity of 0.01 m s^{-1}. The coral cross section is shown as a thick black line.

represent both computational and coral domains with approximately 900,000 cells each with a constant time step.

3. Results and discussion

3.1. Analysis of polyp depths (PD) and surface area to volume (A/ V) ratios

The predicted surface areas and volumes from the proposed model agreed reasonably well with the theoretical results (Table 2) exhibiting low root-mean-square errors (RMSE) between the two measurements. The surface area was defined as the entire area of living coral tissue; the volume was the volume of the entire skeleton plus tissue. Small polyps break up the smooth surface, thereby increasing the coral surface area on a micro-topographical scale. For massive or rounded coral species whose bases contact the reef substrate, only the upper living surface was used in the calculation of their A/V ratios. The A/V ratio of each of the coral species is plotted here against their polyp depths (Fig. 2). These points yield curves that are best represented by exponential functions, where *L. purpurea*: $A/V = 0.33 \cdot e^{0.13 \times PD}$ and *P. sinensis*: $A/V = 0.25 \cdot e^{0.21 \times PD}$. Note that in general, high A/V ratios tend to have deep polyps, and vice versa. The modelled coral morphologies with varying dimple depths up to 5 mm and the corals used by Jimenez et al. (2011) were compared with Porter (1976) observations (Fig. 3). Furthermore, as expected the A/V ratios decreased as the ratio of polyp depth to polyp spacing increased (Fig. 4).

3.2. Coral thermal dynamics and their relationship to PD and A/ V ratios

The effects of maximum irradiance or light capture across the colony due to polyp depths showed that higher polyp depth colonies (or greater A/V ratios) intercepted more light (Fig. 5). Our finding was also consistent with Porter (1976) observation. The small difference in irradiance levels between 1 mm and 5 mm polyp depth for *L. purpurea* and *P. sinensis* were 1.5 and 1.7 W m^{-2}, respectively, and are unlikely to cause any differential surface warming of these colonies.

3.3. Boundary layer thicknesses

The equilibrium surface warming in *L. purpurea*(~2 mm polyp depth) and *P. sinensis*(~1 mm polyp depth) at a flow rate of 0.01 m s^{-1} and ~430 W m^{-2} were 0.39°C and 0.34°C, respectively (Fig. 8). The effective TBL thickness (δ_T) and MBL thickness (δ) of both species increased almost linearly with increasing polyp depth. Temperature differences at the surfaces of these two corals resulted from variations in the thickness of the TBL. In this study, however, the TBL thickness of these two species did not differ substantially. It appears, therefore, that these corals had similar efficiencies regarding convective heat transfer despite their differences in morphology (Fig. 9). TBL thickness ranged from 1.0 to 2.5 mm, whereas MBL thickness was approximately 1.5 and 1.8 times thicker in *L. purpurea* and *P. sinensis*, respectively, which indicates viscous diffusion is expected to be the more dominant process in this case compared to thermal diffusion (Fig. 10).

The simulation results were broadly consistent with the experimental results of Jimenez et al. (2011) with respect to surface warming of polyped coral under steady flow and irradiation. Temperature and irradiance values were obtained for each cells over the entire coral surface area for the simulations, in contrast to the microsensor approach of the experiments (Ong et al., 2018). In the past, gradients of boundary layer conditions for corals have been measured using micro-sensors under laboratory conditions. In contrast, the CFD methods presented here have allowed us to generate a more complete representation of boundary layers that could affect the surface temperatures of corals. Although, laminar boundary layers can readily be measured experimentally, in the presence of turbulence, predicting turbulent boundary layer thicknesses is much more difficult due to the time-dependent variation of the flow properties and smaller thicknesses, and are thus harder to observe experimentally.

3.4. Dimple flow dynamics

The flow patterns due to dimpled surface had little noticeable effect in altering downstream flows (Fig. 11), because flow disturbances remained in the dimples rather than escaping and moving downstream. The wake zone towards the stern of the dimple was characterised by a smaller separation region behind the deeper dimpled surface meaning there is less pressure drag than for a smooth surface due to the low pressure that may draw flow in more due to the rougher surface. A separation line was located at the dimple leading edge and a reattachment line at the trailing edge are similar for both smooth (Ong et al., 2017) and dimpled surfaces.

The present study of thermal performance of dimpled surface in laminar flows shows that there is almost no effect to the overall surface warming compared to smooth surface (Fig. 6) The overall influences of thermal and momentum transport detriments the augmentation of Nusselt number due to the absence of turbulent transport and mixing when the flow is laminar. However, when the flow is turbulent, the overall influences of flow structure and local Nusselt number variations with dimples may affect the flow behaviour and consequently the overall thermal performance (Xiao et al., 2009).

The interspecies differences in coral surface warming modelled here can be attributed to variation in the polyp depth (*PD*), regularity and/or uniformity of polyp surface (polyp diameter and spacing), and area-to-volume (A/V) ratios of colonies. Decreasing the polyp depth resulted in less variation in the heat transfer coefficients across the depth and diameter of the polyp, which in turn, may alter the flow characteristics and increase the heat transfer coefficients. As expected, a small increase in polyp diameter and depth causes an increase in surface area on a micro-topological scale that affects the overall A/V ratio. The simulation results suggest that while differences exist in surface warming between smooth and dimpled surfaces with varying polyp depths (up to 5 mm), they are not substantially different (~0.18–0.19°C) and that these differences can be largely attributed to increasing A/V ratios (Fig. 7).

Therefore, with respect to heat transfer and assuming that heat generated due to the conversion of physiochemical properties is likely to be trivial. It can be assumed that the physiologically integrated massive colonies with smooth-surfaces are likely to replicate similar thermal profiles compared to colonies with polyp-surfaces.

Similarly, species with higher polyp depth are likely to be better suited for light interception and capture because of their greater surface area. This finding also agrees well with theory (Porter, 1976) and field observations in terrestial plants (Horn, 1971; Niklas, 1994) in that colonies with high A/V ratios typically occur in deep water or other low-light environments and often display more open geometries that should also increase the efficiency of light capture, the irradiance intercepted per unit volume (Porter, 1976; D'Elia, 1988; Patterson, 1992). Furthermore, many small polyps should also increase the photosynthetic surface area more than a few large ones, and should therefore be favoured in species with branching morphologies and greater A/V ratios. In addition, massive or plate-like species, whose bases contact the reef or seafloor, only their upper living surface tissue intercepts light. Therefore, although species with higher polyp depth or A/V ratios are likely to accumulate more solar irradiance which in turn generate slightly greater thermal stress, they may be more energetically favourable due to higher procurement of nutrients and energy through symbiosis.

Temperature differences of coral surfaces may also be attributable to variations in the thickness of the TBL. However, in this study, various TBL thicknesses were associated with similar efficiencies of convective heat transfer. The convection coefficient can be expressed as an inverse relationship of the thickness of the TBL ($h = k/\delta_{TBL}$), rearranging Equations (2) and (3), the warming can be written as:

$$\Delta T = \frac{\delta_{TBL}\, I\, \alpha}{k_m} \tag{19}$$

Therefore, for a given irradiance (I), the slope of the relationship between warming (ΔT) and TBL thickness (δ_{TBL}) should be proportional to the coral absorptivity (α), and inversely proportional to the thermal conductivity of water and coral ($k_m = (1 - \varphi)k_c + k_w$). Thus, thermal properties of both the tissue and skeleton regions, and morphological traits such as the size and shape of the colony, may directly affect the thermal dynamics of coral microenvironments.

Presently, the effects on flow of various shapes of coral polyps are largely unexamined. However, a variety of physical parameters and ratios including polyp diameter and depth, polyp depth to diameter ratio, polyp depth to spacing ratio, Reynolds numbers associated with different conditions, and the many possible combinations thereof, are all likely important determinants of thermal dynamics at microscales around corals. Furthermore, because morphological variation in corals can be strongly influenced by light/irradiance and water flow rates (Helmuth et al., 1997; Anthony et al., 2004; Berkelmans et al., 2004), the coral thermal microenvironments are likely to have profound implications not only in the context of thermal stress but also in relation to many other temperature-controlled processes, such as rates of metabolism and growth. For example, skeletons of massive *Porites sp.* are widely used as proxies of past and present SST (Barnes et al., 1989; Barnes and Lough, 1993, 1999). Their rates of linear extension increase by 27% of the mean with each 1°C warming (Lough and Barnes, 2000). The thermal microenvironment can be defined as the temperature of the colony surface and of the boundary layer directly above it, which can deviate substantially from the mean temperature of the surrounding seawater. This temperature deviation is a function of several factors, though it is predominantly due to radiative heat flux and water flow on the coral surface. A heat balance is maintained between losses from convection into the surrounding water (dependent on water flow and other surface characteristics involved in the boundary layer formation), heat conduction into deeper layers of the coral, and emission of short and long-wave radiation incident on the coral surface (Fabricius, 2006). Moreover, this relationship would likely become even more complex given the expected dependence of coral surface temperatures on pigmentation and area of percolation through openings and increased porosity due to grazers or predators (Ong et al., 2012).

4. Conclusion

In summary, this study investigated the effects of coral thermal microenvironments between the smooth- and polyped-surface under a steady laminar water currents and constant irradiance of ~430 W m^{-2}. The results suggest that while differences exist in surface warming between smooth and dimpled surfaces with varying polyp depths (up to 5 mm), but the variation is not distinct (~0.18°C) which could be largely attributed to the difference in their surface area-to-volume (A/V) ratios. From a heat transfer perspective, physiologically integrated smooth-surfaced massive colonies can be appropriate for modelling the thermal profiles of colonies consisting of modular polyps. Moreover, the interspecies difference considered here appear equally effective in terms of light modulation to achieve similar irradiance levels. We also shown that numerical results from CFD is able to resolve energy transport and TBL conditions and compare well with the experimental study of Jimenez et al. (2011).

Author contributions

Conception and design of the study: R.H.O., A.J.K., B.J.M. and M.J.C.; R.H.O. and A.J.K. performed the simulations; R.H.O., A.J.K., B.J.M and M.J.C. analyzed the data; R.H.O., A.J.K., B.J.M and M.J.C. interpreted the results; R.H.O. and A.J.K. prepared the figures and drafted the manuscript. All authors critically revised the manuscript and approved the final version.

Declaration of competing interest

The authors declare they have no actual or potential competing financial and non-financial interests.

Acknowledgements

The authors wish to thank Dr. Tim Cooper who formerly worked at the Australian Institute of Marine Science and the UWA Ocean Institute. The authors acknowledge Pawsey Supercomputing Center for access to its high performance computing infrastructure. We also acknowledge the OpenFOAM community and developers.

Appendix A. Supplementary data

Supplementary data to this article can be found online at https://doi.org/10.1016/j.jtherbio.2019.102433.

References

Anthony, K.R.N., Ridd, P.V., Orpin, A.R., Larcombe, P., Lough, J., 2004. Temporal variation of light availability in coastal benthic habitats: effects of clouds, turbidity, and tides. Limnol. Oceanogr. 2201–2211.
Barnes, D.J., Lough, J.M., 1993. On the nature and causes of density banding in massive coral skeletons. J. Exp. Mar. Biol. Ecol. 167, 91–108.
Barnes, D.J., Lough, J.M., 1999. Porites growth characteristics in a changed environment: misima island, Papua New Guinea. Coral Reefs 18, 213–218.
Barnes, D.J., Lough, J.M., Tobin, B.J., 1989. Density measurements and the interpretation of x-radiographic images of slices of skeleton from the colonial hard coral porites. J. Exp. Mar. Biol. Ecol. 131, 45–60.
Berkelmans, R., De'ath, G., Kininmonth, S., Skirving, W.J., 2004. A comparison of the 1998 and 2002 coral bleaching events on the great barrier reef: spatial correlation, patterns, and predictions. Coral Reefs 23, 74–83.
Brandt, M., 2009. The effect of species and colony size on the bleaching response of reef-building corals in the Florida keys during the 2005 mass bleaching event. Coral Reefs 28, 911–924.
Cooper, T.F., 2008. Coral Bioindicators of Environmental Conditions on Coastal Coral Reefs. Ph.D. thesis. James Cook University.

D'Elia, C.F., 1988. The cycling of essential elements in coral reefs. In: Concepts of Ecosystem Ecology. Springer, pp. 195–230.
Dunne, R., Brown, B., 2001. The influence of solar radiation on bleaching of shallow water reef corals in the andaman sea, 1993–1998. Coral Reefs 20, 201–210.
Fabricius, K.E., 2006. Effects of irradiance, flow, and colony pigmentation on the temperature microenvironment around corals: implications for coral bleaching? Limnol. Oceanogr. 51, 30–37.
Ferziger, J.H., Perić, M., 1999. Computational Methods for Fluid Dynamics. Springer, Berlin.
Glynn, P.W., 1990. Coral mortality and disturbances to coral reefs in the tropical eastern pacific. Elsevier Oceanogr. Ser. 52, 55–126.
Glynn, P.W., 1996. Coral reef bleaching: facts, hypotheses and implications. Glob. Chang. Biol. 2, 495–509.
Guest, J.R., Baird, A.H., Maynard, J.A., Muttaqin, E., Edwards, A.J., Campbell, S.J., Yewdall, K., Affendi, Y.A., Chou, L.M., 2012. Contrasting patterns of coral bleaching susceptibility in 2010 suggest an adaptive response to thermal stress. PLoS One 7, e33353.
Helmuth, B.S., Sebens, K.P., Daniel, T.L., 1997. Morphological variation in coral aggregations: branch spacing and mass flux to coral tissues. J. Exp. Mar. Biol. Ecol. 209, 233–259.
Hoegh-Guldberg, O., 1999. Climate change, coral bleaching and the future of the world's coral reefs. Mar. Freshw. Res. 50, 839–866.
Horn, H.S., 1971. The Adaptive Geometry of Trees, vol. 3. Princeton University Press.
Jimenez, I., Kuhl, M., Larkum, A., Ralph, P., 2008. Heat budget and thermal microenvironment of shallow-water corals: do massive corals get warmer than branching corals? Limnol. Oceanogr. 53, 1548–1561.
Jimenez, I.M., Kühl, M., Larkum, A.W., Ralph, P.J., 2011. Effects of flow and colony morphology on the thermal boundary layer of corals. J. R. Soc. Interface 8, 1785–1795.
Joshi, K.B., 2013. Modeling of Bio-Inspired Jellyfish Vehicle for Energy Efficient Propulsion (Ph.D. thesis).
Lough, J., Barnes, D., 2000. Environmental controls on growth of the massive coral porites. J. Exp. Mar. Biol. Ecol. 245, 225–243.
Loya, Y., Sakai, K., Yamazato, K., Nakano, Y., Sambali, H., Van Woesik, R., 2001. Coral bleaching: the winners and the losers. Ecol. Lett. 4, 122–131.
Marshall, P., Baird, A., 2000. Bleaching of corals on the great barrier reef: differential susceptibilities among taxa. Coral Reefs 19, 155–163.
Moberg, F., Folke, C., 1999. Ecological goods and services of coral reef ecosystems. Ecol. Econ. 29, 215–233.
Mumby, P.J., Chisholm, J.R., Edwards, A.J., Andrefouet, S., Jaubert, J., 2001. Cloudy weather may have saved society island reef corals during the 1998 enso event. Mar. Ecol. Prog. Ser. 222, 209.
Nakamura, T., Van Woesik, R., Yamasaki, H., 2005. Photoinhibition of photosynthesis is reduced by water flow in the reef-building coral acropora digitifera. Mar. Ecol. Prog. Ser. 301, 109–118.
Nakamura, T., Yamasaki, H., Van Woesik, R., 2003. Water flow facilitates recovery from bleaching in the coral stylophora pistillata. Mar. Ecol. Prog. Ser. 256, 287–291.
Niklas, K.J., 1994. Plant Allometry: the Scaling of Form and Process. University of Chicago Press.
Ong, R.H., King, A.J., Caley, M.J., Mullins, B.J., 2018. Prediction of solar irradiance using ray-tracing techniques for coral macro-and micro-habitats. Mar. Environ. Res. 141, 75–87.
Ong, R.H., King, A.J.C., Kaandorp, J.A., Mullins, B.J., Caley, M.J., 2017. The effect of allometric scaling in coral thermal microenvironments. PLoS One 12, 1–27.
Ong, R.H., King, A.J.C., Mullins, B.J., Cooper, T.F., Caley, M.J., 2012. Development and validation of computational fluid dynamics models for prediction of heat transfer and thermal microenvironments of corals. PLoS One 7, e37842.
OpenCFD Ltd, 2010. OpenFOAM - User Guide. OpenCFD Ltd. Version 1.7. http://www.openfoam.com/.
Patankar, S.V., 1980. Numerical Heat Transfer and Fluid Flow: Computational Methods in Mechanics and Thermal Science. Hemisphere Publishing Corp.
Patterson, M.R., 1992. A chemical engineering view of cnidarian symbioses. Am. Zool. 32, 566–582.
Porter, J.W., 1976. Autotrophy, heterotrophy, and resource partitioning in caribbean reef-building corals. Am. Nat. 731–742.
Shenkar, N., Fine, M., Loya, Y., 2005. Size matters: bleaching dynamics of the coral oculina patagonica. Mar. Ecol. Prog. Ser. 294, 181–188.
Teneva, L., Karnauskas, M., Logan, C.A., Bianucci, L., Currie, J.C., Kleypas, J.A., 2012. Predicting coral bleaching hotspots: the role of regional variability in thermal stress and potential adaptation rates. Coral Reefs 31, 1–12.
Veron, J., 1995. Corals in Space and Time: the Biogeography and Evolution of the Scleractinia. Cornell University Press.
Veron, J., 2000. Corals of the World, vols. 1–3. Australian Institute of Marine Science.
Versteeg, H., Malalasekera, W., 1995. An Introduction to Computational Fluid Dynamics: the Finite Volume Approach (Longman Scientific, Technical).
van Woesik, R., Irikawa, A., Anzai, R., Nakamura, T., 2012. Effects of coral colony morphologies on mass transfer and susceptibility to thermal stress. Coral Reefs 1–7.
Xiao, N., Zhang, Q., Ligrani, P.M., Mongia, R., 2009. Thermal performance of dimpled surfaces in laminar flows. Int. J. Heat Mass Transf. 52.